

SCANNING AIRBORNE DOPPLER RADAR

Lin Tian^{1,2}Gerald M. Heymsfield², Stephen Guimond³, Lihua Li², Ramesh Srivastava⁴¹Morgan State University/GESTAR, ²NASA Goddard Space Flight Center,
³Oak Ridge Associated Universities, ⁴University of Chicago**1. Introduction**

Doppler radars flying on high altitude (18 – 20 km) aircraft for the observation of tropical storms have capability to estimate wind and precipitation fields simultaneously at fine spatial resolutions. Over the past decade, the nadir-viewing ER-2 Doppler radar (EDOP) has flown over many intense convective storms while directly measuring the vertical mean Doppler velocity relative to the aircraft (e. g. Heymsfield et al. 2010). Those observations along with data from other remote sensing instruments on the ER-2 have contributed to a better understanding of kinematic, microphysical and even thermodynamic processes leading to the formation, maintenance, and evolution of hurricanes and deep convective storms.

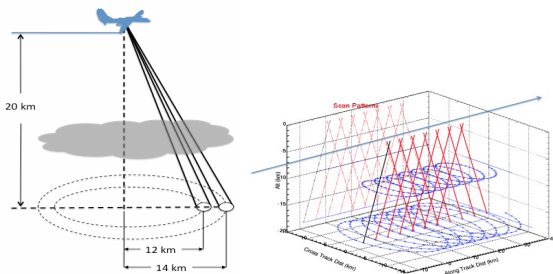


Fig. 1 a) Schematic of HIWRAP scanning geometry; b) beam trajectory (blue) at two different heights.

A nadir-looking airborne radar can provide observations only in the vertical plane along the flight path. Recently, a new airborne radar, HIWRAP (High-Altitude Imaging Wind and Rain Airborne Profiler), has been developed at NASA

Goddard Space Flight Center for measuring three-dimensional reflectivity and wind fields within precipitation regions and ocean surface winds in rain-free regions (Li et al. 2008). In contrast to EDOP, a single frequency radar with two fixed beams pointing to nadir and forward, HIWRAP has two frequencies (14 and 35 GHz), and scans conically with 30° and 40° incidence angles. The two frequencies of HIWRAP are the same as the upcoming GPM dual-frequency radar so the data is valuable for GPM algorithm development. The dual-wavelength reflectivities could help reduce the uncertainty in rain estimation due to the variability of the particle size distribution. Doppler velocities from HIWRAP could provide wind information not only in the vertical along-track plane but also in other planes aligned to the flight track. Such observations are needed for advancing our understanding of hurricane inner core structures and intensification.

The HIWRAP flew on NASA's Global Hawk (an unmanned aircraft) for the first time in the summer of 2010 during the NASA GRIP (Genesis and Rapid Intensification Process) field experiment. This paper will focus on the feasibility of using Doppler velocity from HIWRAP for 3D wind retrieval. In the following, we will first describe the HIWRAP instrumentation and its capabilities. In section 3, we will present wind retrieval methods applicable to the HIWRAP. Some initial results will be presented in section 4.

2. HIWRAP measurements

The scans of HIWRAP are similar to PPI scans from a ground-based radar but looking downwards. The system specifications of HIWRAP are given in Table 1. As the aircraft moves, the radar beams sweep out two spiral paths. Figure 1 shows the radar beam trajectory (in blue) at two different heights for one incidence angle. The beam trajectory at time t is given by

Corresponding author address: Lin Tian, Mesoscale Atmospheric Process Branch, NASA Goddard Space Flight Center, Code 613.1, Greenbelt, MD 20771;email: lin.tian-1@nasa.gov

$$x = R \sin(\beta) = R \sin(\Omega t) \quad (1)$$

$$y = U_A t + R \cos(\beta) = U_A t + R \cos(\Omega t) \quad (2)$$

where

x = across track distance

y = distance along aircraft track

U_A = aircraft speed, constant

β = azimuth angle of conical scan measured

counter-clockwise from x – axis

α = beam angle from the vertical

R = radius of scan circle = $h \tan \alpha$

h = depth (vertical) of scan plane below the aircraft

Ω = antenna rotation rate (CCW) of antenna, radians per second

TABLE 1. HIWRAP SYSTEM SPECIFICATIONS

Parameters	Specifications	
	Ku-band	Ka-band
RF Frequency (GHz)	Inner Beam: 13.910 Outer Beam: 13.470	Inner Beam: 35.560 Outer Beam: 33.720
Tx Peak Power (W)	30	10
Beam Width ($^\circ$)	2.9	1.2
Beam Pointing Angle ($^\circ$ off nadir)	30 (inner), 40 (outer)	
Polarization	H (inner beam), V (outer beam)	
PRF (Hz)	0-5000	
Tx Pulsewidth (μ s)	0-40	
Range Bin (m)	37.5-150	
Detection Range (km)	0-30	
Minimum Detect. Reflectivity (dBZ _e , 60 m range res., 10 km range and 3 km chirp pulse)	0.0	-5.0
Dynamic Range (dB)	> 65	
Doppler Velocity (ms ⁻¹)	0-150 (Accuracy < 1.5 ms ⁻¹ for SNR>10)	
Scanning	Conical Scan, 16 rpm	

From the trajectories it is clear that many observations are obtained at coincident points (i.e., the points of intersections of the circles). These observations are also temporally very close because the time to complete one revolution of the antenna is short, nominally 3.5 seconds. This should provide greater accuracy in combining the Doppler velocities to obtain wind vectors.

3. Method for 3D wind retrieval for HIWRAP

HIWRAP provides a 3D view of tropical storms. However, the 3D Doppler data from multiple locations, as the plane flies, does not necessarily guarantee that we can retrieve 3D wind fields. If the plane flies in a straight line, we obtain essentially data for dual-Doppler analyses by combining fore and aft looks and the 3D wind synthesis is not possible unless additional constraints are available. Also, for HIWRAP, it is not feasible to use the data collected from “L” shaped flight patterns, which have been used for airborne radars when the scanning axis is oriented parallel to the flight track, e.g. NOAA’s tail radar on P3 and NCAR ELDORA (Jorgensen et al. 1983). This is because the antenna elevations angles of HIWRAP are presently fixed at -60° for the inner beam and -50° for the outer beam, and therefore the common areas covered by the two legs of the L-shaped flight path are too small for meaningful analysis. Note that the convention for elevation angle is the same as that for ground-based radars. Negative elevation means the radar is looking down. In the following, we will develop the equations for dual-Doppler analysis for HIWRAP scanning geometry followed by the equations for VAD analysis.

a) Dual-Doppler Analysis

In principle, dual-Doppler synthesis that is well-established for ground-based scanning Doppler radars can be applied to HIWRAP for wind retrievals once the Doppler velocity is corrected for velocity folding and aircraft motion. For HIWRAP scanning geometry, we can derive the wind components parallel and perpendicular to the flight track in planes with one axis along the flight track. This can be illustrated with a cylindrical coordinate system (Fig. 2). This is similar to the co-plane method (Armijo1969) used by ground-based radars except that for HIWRAP the co-plane angle is zero in the vertical plane under the flight track.

In the following discussion, we assume the data has been corrected for aircraft motion and interpolated onto a common grid (x_i, y_i, z_i) with y_i along the flight track, x_i perpendicular to y_i , and z_i in the vertical. For details on mapping the data from aircraft coordinate to track-relative coordinate, see Lee et al. (1993).

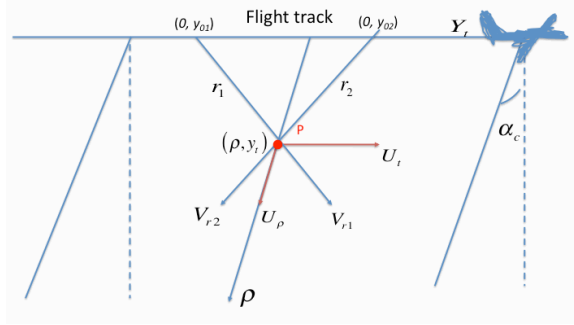


Fig. 2 Cylindrical coordinates system used for dual-Doppler radar analysis. Radar is located at points y_{01} and y_{02} , y_t, ρ and α_c are the cylindrical axis along the flight track, range from the axis to grid point P, and colplan angle, respectively. V_{r1} and V_{r2} are the mean radial Doppler velocities at grid point P, and U_ρ , and U_t are the wind components on the colplan. U_α is the wind components perpendicular to the coplan.

At any grid point (x_t, y_t, z_t) and time t , radial mean Doppler velocity is given by

$$V_r = \frac{ux_t + v(y_t - y_0) + z_t W}{r} \quad (3)$$

where $W = w - V_T$ and $y_0 = U_a t$.

where (u, v, w) are the wind components in x_t, y_t and z_t direction, r is the range from radar, and V_t is the terminal velocity of the hydrometeors. U_a is the speed of the aircraft.

In a cylindrical coordinate system (Fig. 2) with flight track as axis y_t and ρ as the axis perpendicular to the flight track, and U_ρ as the wind component in ρ direction, eq. (5) can be written as

$$V_r = \frac{\rho}{r} U_\rho + \frac{y_t}{r} v \quad (4)$$

$$U_\rho = u \sin \alpha_c - W \cos \alpha_c \quad (5)$$

$$r = \sqrt{\rho^2 + (y_t - y_0)^2} \quad (6)$$

Where α_c is the coplan angle. Note that the cross track component contains both u and W . In the nadir plan, $\alpha_c = 0$, $U_\rho = -W$ the wind component in the vertical. From Doppler velocities measured

by HIWRAP at positions y_{01} and y_{02} along the flight track, we have

$$V_{r1} = \frac{\rho}{r_1} U_\rho + \frac{(y_t - y_{01})}{r_1} v \quad (7)$$

$$V_{r2} = \frac{\rho}{r_2} U_\rho + \frac{(y_t - y_{02})}{r_2} v \quad (8)$$

From (7) and (8), we have

$$U_\rho = \frac{r_1 (y_t - y_{02}) V_{r1} - r_2 (y_t - y_{01}) V_{r2}}{-\rho (y_{02} - y_{01})} \quad (9)$$

$$v = \frac{r_1 V_{r1} - r_2 V_{r2}}{(y_{02} - y_{01})} \quad (10)$$

Assuming V_{r1} and V_{r2} are independent, the variance of U_ρ and v are given by

$$\sigma_{U_\rho}^2 = \left[\frac{r_1 (y_t - y_{02})}{\rho (y_{02} - y_{01})} \right]^2 \sigma^2(V_{r1}) + \left[\frac{r_2 (y_t - y_{01})}{\rho (y_{02} - y_{01})} \right]^2 \sigma^2(V_{r2}) \quad (11)$$

$$\sigma_v^2 = \left(\frac{r_1}{y_{02} - y_{01}} \right)^2 \sigma^2(V_{r1}) + \left(\frac{r_2}{y_{02} - y_{01}} \right)^2 \sigma^2(V_{r2}) \quad (12)$$

where $\sigma^2(V_{rj}), j=1,2$ is related to the errors in mean Doppler velocity which include 1) signal fluctuations; 2) residual in aircraft motion correction; 3) antenna pointing error. The other terms in bracket are geometrical factors. In the nadir plane, we have

$$v = \frac{V_{r1} - V_{r2}}{2 \cos \alpha} \quad (13)$$

$$W = \frac{V_{r1} + V_{r2}}{2 \sin \alpha} \quad (14)$$

$$\sigma^2(v) = \frac{\sigma^2(V_r)}{2 \cos^2 \alpha} \quad (15)$$

$$\sigma^2(W) = \frac{\sigma^2(V_r)}{2 \sin^2 \alpha} \quad (16)$$

where α is the track relative incidence angle from nadir which could be slightly different from the incidence angle relative to aircraft depending on the roll and pitch of the aircraft. So at nadir we can use forward and aft looks from two different scans to calculate the v and W . The assumption is that the time difference between the two radial velocities at the intersections is small. For HIWRAP inner beams, the time difference between the fore and aft beams viewing the same volume are about 131, 98, 65, and 32 seconds at heights of 0, 5, 10, 15 km assuming the aircraft flew at 20 km altitude with a speed of 176 m/s.

The corresponding time difference for outer beams is about 190, 143, 95, and 48 seconds. In general, the standard error due to signal fluctuations is small. Using the HIWRAP radar parameters in Table 1, we estimated standard errors in mean Doppler due to signal fluctuations to be $\sigma(V_r) = 0.18$ for Ku band and 0.09 m/s for Ka band. For $\alpha = 30$ deg, $\sigma(v) = 0.15$ for Ku and 0.07 m/s for Ka. Substitute those number into eq (15) and (16), we have $\sigma(W) = 0.25$ for Ku and 0.13 for Ka. For alpha = 40 deg, $\sigma(v) = 0.17$ for Ku and 0.08 m/s for Ka. $\sigma(W) = 0.2$ for Ku and 0.1 m/s for Ka. The largest errors are due to errors in the aircraft motions.

Using the radar data collected at intersecting grid points from two locations along the flight path, we can estimate cross-track wind components along axis ρ , U_ρ , and along track component, U_t . In the vertical plane under the flight track, U_ρ becomes the vertical wind, and we cannot get the wind component perpendicular to the coplane, which is cross-track. For ground-based dual-Doppler analysis, the wind component perpendicular to coplanes is estimated by integrating the continuity equation. This requires knowledge of the wind component perpendicular to a coplane. This is provided by the condition $w = 0$ imposed at or near the ground, which happens to be a coplane. For HIWRAP, the surface, or near surface plane, is not a coordinate plane, or a coplane, of the cylindrical coordinate system. Therefore, application of the continuity constraint is not straightforward. A technique for applying the continuity equation will be presented in a future contribution. The separation of cross-track and W components will be investigated further. Regardless of this limitation, wind components along the track and in the vertical can be determined unambiguously and they are important not only for hurricane research but also useful for evaluating the linear wind assumption used in VAD analysis, which is discussed next.

b) VAD analysis

VAD (velocity azimuth display) analysis has been used to determine the vertical profiles of horizontally uniform, or linearly varying, wind (e.g. Lhermitte and Atlas 1961) from single ground-based Doppler radar. Before applying this method to HIWRAP measurements, we first interpolate data from each scan data at 5° azimuth interval in

track coordinats after removing the aircraft motion from Doppler velocity. We then average 5 scans for a given azimuth assuming that variations of radar observations within 5 scan volumes are small and the centers of the VAD circles are fixed for any given scan. With HIWRAP's nominal rotation rate of 96° /s, the center of the scan circle moves 0.65 km when radar completes one 360° scan and 3.27 km for 5 scans. We assume that wind is linear inside each "VAD volume". Depending upon the meteorological situation, this assumption may be reasonable for stratiform rain but probably not for convective rain, or inside a hurricane. With these assumptions, the equations for VAD analysis for HIWRAP are similar to those used for ground-based radar.

$$V_r(\beta) = u \cos \alpha \sin \beta + v \cos \alpha \sin \beta + W \sin \alpha \quad (17)$$

where α and β are elevation and azimuth angles. Assuming linear wind in each VAD circle along the track we have

$$\begin{aligned} u &= u_0 + u_x x_t + u_y y_t \\ v &= v_0 + v_x x_t + v_y y_t \\ W &= W_0(z_t) \end{aligned} \quad (18)$$

Substitute above equations into (17) we have

$$V_r(\beta) = a_0 + a_1 \cos \beta + a_2 \sin \beta + b_1 \cos(2\beta) + b_2 \sin(2\beta) \quad (19)$$

If the radius of VAD circle $R = r \cos \alpha$, where r is the range from radar to the target, we have

$$\begin{aligned} a_0 &= W_0 \sin \alpha - \text{DIV} \frac{R \sin \alpha}{2} \\ a_1 &= u_0 \cos \alpha, \quad a_2 = v_0 \cos \alpha \end{aligned} \quad (20)$$

where DIV is the divergence of the horizontal wind. b_1 and b_2 are related to the deformation of horizontal wind. Subscripts x, y, z in eq. 18 denote partial derivatives. We can estimate coefficients $a_i, i = 0, 1 \dots 4$ using least squares fitting. For the ground-based radars with low elevations angles, the vertical velocity and divergence are determined by combining eq. (20) and the continuity equation with a boundary condition used for vertical air velocity at the cloud top or bottom. For HIWRAP, we will use the nadir vertical velocity derived from dual-Doppler analysis and eq. (20) to calculate divergence.

4. Results

HIWRAP data from tropical storm Matthew collected on 24 Sep 2010 was used for testing the wind retrieval methods. This is one of the best data sets in terms of data quality after problems with digital receiver on prior flights were resolved. A convective burst began right before the Global Hawk arrived in the area and was sustained throughout the flight. Matthew intensified by 5 - 10 knots during the flight, reaching a peak intensity of 50 knots around 1800 UTC. The storm was unable to intensify beyond wind speed of 50 knots but it went on to produce more than 16 inches of rain in parts of Yucatan, Mexico. Figure 3 shows flight lines of the Global Hawk overlaid on the GOES IR image of Matthew.

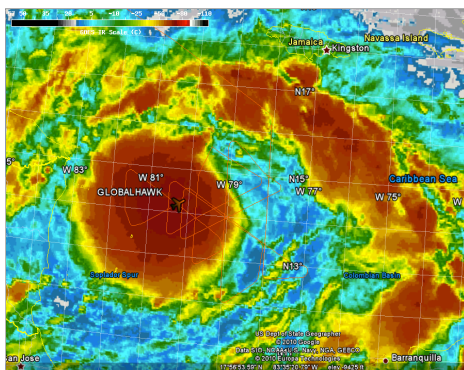


Fig. 3. Flight lines of Global Hawk overlay on GOES IR image on Sep 24 2010.

Combining antenna rotation rate with the aircraft's nominal ground speed (176 m/s) results in a horizontal resolution of approximately 0.65 km. The range resolution is 0.150 km. The horizontal area covered near the surface is within ± 12 km (30° beam) and ± 17 km (40° beam) of the flight track. Raw real and imaginary (I and Q) data were collected onboard and saved every two minutes. Pulse compression using a pulse length of $20 \mu s$ is used to achieve the desired range resolution and sensitivity. Pulse-pair processing was applied to the raw I and Q to get the return power and Doppler velocity using 64 samples. The final processing merges the radar data along with the aircraft navigation data, the antenna rotation angles, corrects Doppler velocity for aircraft motion and velocity folding.

Fig. 4a shows an example of one flight line at 0713-0718 UTC on 24 Sep 2011. We plot the vertical cross-section for the fore and aft beams separately. The observed reflectivity from fore and aft looks are quite similar. The melting band is at

about 4.8 km height. A convective rain band occurs at around 7:23 UTC. The slight difference in height is because antenna is tilted up slightly so the track-relative elevation varies with azimuth. The difference at beginning is due to aircraft roll during turns. The locations of the stratiform and convective regions are also shown in the brightness temperature observed at 89 GHz from the radiometer on Aqua satellite (Fig. 4b).

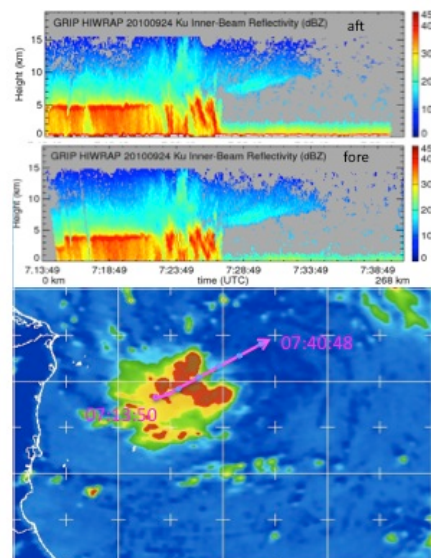


Fig. 4. Matthew flight: a) Vertical cross-section of HIWRAP Ku-band reflectivity from aft (top) and forward (middle) beams during 0713 - 0738 UTC 24 Sep 2010; b) Composite image of brightness temperature at 89 GHz from AQUA-1 at 0708Z and GOES IR temperature at 0715 UTC (bottom). (<http://www.nrlmry.navy.mil/tc.html>). The blue line shows the flight track of Global Hawk.

a) Vertical and along track wind at nadir

For estimation of nadir winds, we interpolated the data onto a track-relative coordinate as described in Section 3a. Data from the forward and aft looks are plotted separately. By comparing the data from the forward and aft looks, we can determine if the storm structure changed over the time period that it took for the fore and aft beams to intersect. A change could affect the wind estimated from radial mean Doppler velocity of the fore and aft beams. Figure 5 shows the radial Doppler velocities from the fore and aft beams. They differ from each other because the true velocities are projected on different radials. Note that positive Doppler is toward radar (upward) and negative is away from the radar (downward). In the stratiform region, we see mostly downward

Doppler velocity because of falling raindrops. The vertical wind in the stratiform region is small in general. In the convective region, we see relatively strong upward motion from forward beam and downward motion from aft beam.

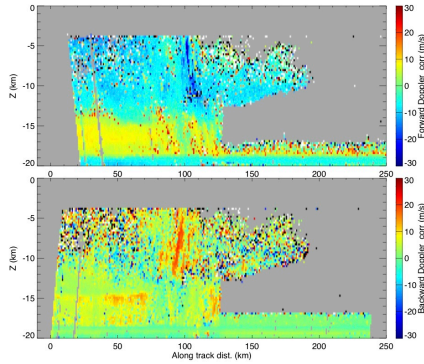


Fig. 5 Radial Doppler velocity from fore (top panel) and aft (bottom panel) beam at Ku-band inner beam. Positive is away from radar (downward) and negative is toward the radar (upward).

Figure 6 shows calculated vertical and horizontal velocities at nadir using the dual-Doppler analysis method described in Sec. 3a. Note that the vertical velocity shown in Fig. 6 is $w-V_t$. We will discuss estimation of V_t in a future contribution. In the convective region, the figure shows a strong updraft of about 10 m/s accompanied by a downdraft of about the same magnitude above the freezing level (located at $z = -15$ km). In the stratiform rain, we see downdrafts of less than 10 m/s assuming $V_t \sim 5$ m/s.

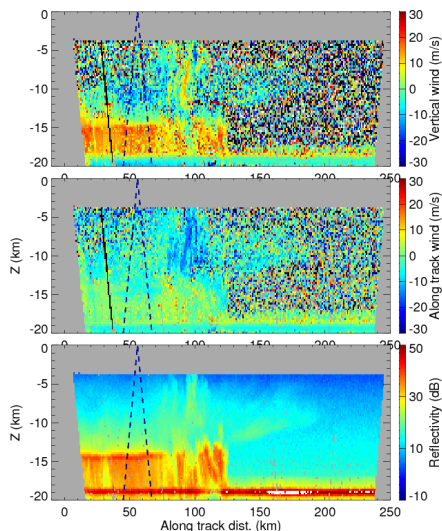


Fig. 6 From top to bottom: $w-V_t$; along-track wind calculated from fore and aft beams using dual-Doppler analysis; averaged reflectivity from fore and aft beam. The triangle enclosed by dash line shows the area covered by one scan for the inner beam.

b) Results from VAD analysis

For testing VAD analysis, we selected an area with uniform stratiform rain. The dashed triangle in fig. 6 shows the vertical and horizontal extent of height covered by one VAD volume. At 3 km height, the radius of VAD circle is about 10 km.

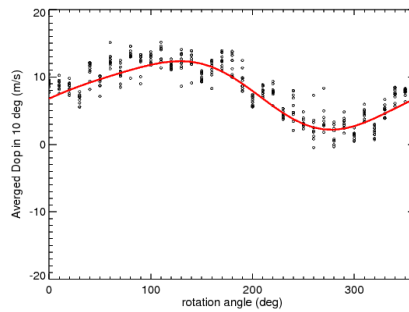


Fig. 7 Averaged Doppler velocity in 10 degree intervals from ten scans centered around 56 km distance. The red line is the least squares fitting using one of the circle in the fig assuming $w-V_t = 15$ m/s, $z = -15.75$ km.

Figure 7 shows the mean Doppler velocities measured by HIWRAP's inner beam along ten VAD circles at height of 3 km. Superposed on the usual VAD sinusoidal curves are some regular fluctuations. These could be due to regular variations in scan elevation angle, or from pronounced waves in the flow. Those will be investigated in the future. To reduce the random fluctuations we have averaged the Doppler on each VAD circle in 10° azimuth, followed by average of 5 scans.

Figure 8 shows the vertical profiles of derived wind fields. The solid black and dark blue lines are the $w-V_t$ and along track wind calculated from dual-Doppler analysis, averaged within the VAD volume. The along-track wind estimated from VAD analysis (dark blue dash in Fig. 7) compares reasonably well with that from dual-Doppler analysis (dark blue solid). The large discrepancy occurs near the melting layer where the precipitation is uniform. Cross-track wind (light blue line in Fig. 8) is about 10 m/s below the

melting layer and near zero at higher level. This is consistent with the general wind direction (counter clock wise rotation) of tropical storm Matthew in Fig. 4b. Note that direction of the cross-track wind is defined as positive when wind is pointing on the right of the flight track, or towards the southeast for this flight line. Figure 9 shows the divergence calculated from w-Vt and VAD fitting using coefficient a_0 .

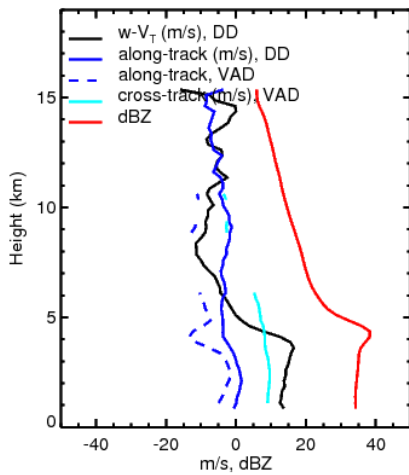


Fig. 8 Vertical profiles of W-Vt, along track wind, and reflectivity from all profiles within the triangle shown in Fig. 1. The aircraft flew at an altitude of 18.86 km. For comparison, the blue dash line shows the along-track wind and light blue solid line shows are estimated from VAD analysis.

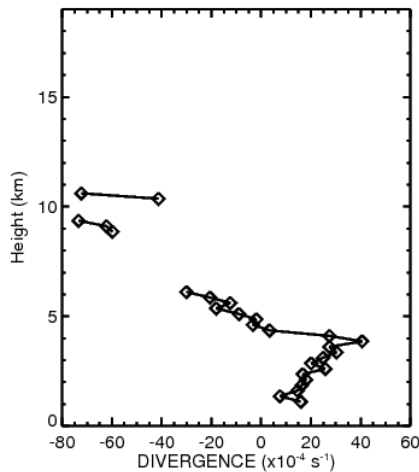


Fig. 9 the divergence calculated from w-Vt and VAD fitting using coefficient a_0 .

5. Summary and Conclusion

A new airborne dual-wavelength Doppler radar, High-Altitude Imaging Wind and Rain

Airborne Profiler (HIWRAP), has been developed at NASA Godard. Unlike the ER-2 Doppler radar (EDOP) which has fixed antennas, HIWRAP scans downward conically with two different elevation angles. The conical scanning capability of HIWRAP greatly extended the capability of EDOP and provides us a great opportunity for estimating wind field inside the storm not only in the nadir under the flight track, but also away from the track. In this paper, we have explored the feasibility of combining dual-Doppler synthesis with VAD analysis for 3D wind retrieval using data collected during NASA GRIP mission. We conclude that 1) The dual-Doppler synthesis is applicable for mapping the wind field in the vertical cross-section under the flight track to a high degree of accuracy if Doppler velocity has been properly corrected for aircraft motion and antenna pointing errors; and 2) the horizontal wind fields can be calculated in the stratiform assuming a horizontally linear wind field. Testing on actual data shows a general agreements in along track wind between dual-Doppler and VAD analysis. To calculate the divergence using VAD analysis, we have used vertical velocity derived from the Dual-Doppler synthesis.

Acknowledgements. We would like to thank Matthew McLinden, and Jaime C. for processing the data, Martin Perrine and Ed Zanker for Engineer supports.

References

- Armijo, L., 1969: A theory for the determination of wind and precipitation velocities with Doppler radars, *J. Atmos. Sci.* **26**, 570-575.
- Heymsfield, G. M., L. Tian, A. J. Heymsfield, L. Li, Steven Guimond, 2010: Characteristics of deep convection from nadir-viewing high-altitude airborne Doppler radar, *J. Atmos. Sci.*, **67**, 285-308.
- Jorgensen, D. P., P. H. Hildebrand, and C. L. Frush, 1983: Feasibility test of an airborne pulse-Doppler meteorology radar. *J. Climate Appl. Meteor.*, **22**, 744-757.
- Lee, W.-C., P. Dodge, F. D. Marks, and P.H. Hildebrand, 1994: Mapping of airborne Doppler radar data. *Atmos. Oceanic Technol.*, **11**, 572-578.
- Lhermitte, R. M., and Atlas, D. 1961: Precipitation motion by pulse Doppler radar. Proc. Weather Radar Conf., 9th, 1961 pp., 218-223.
- Li, L., G. M. Heymsfield, J. Carswell, D. Schaubert, J. Creticos, M. Vega, 2008: High-Altitude Imaging Wind and Rain Airborne

Radar (HIWRAP), Proceedings of IGARSS
2008 (IEEE International Geoscience &

Remote Sensing Symposium), Boston, MA,
USA, July 6-11, 2008.